

The 2012 North Atlantic Hurricane Season

A Climate Perspective

Gerald Bell¹, Stanley Goldenberg², Eric Blake³, Chris Landsea³,
 Jae Schemm¹, Richard Pasch³, Todd Kimberlain³

¹ Climate Prediction Center/ NOAA/NWS/NCEP

² Hurricane Research Division/NOAA/OAR/AOML

³ National Hurricane Center/NOAA/NWS/NCEP

Contents:	
1. 2012 Seasonal Activity	pp. 1-2
2. NOAA's 2012 Seasonal Hurricane Outlooks	pp. 2-3
3. Atlantic Named Storm Tracks during 2012	pp. 3-5
4. Atlantic Sea Surface Temperatures (SSTs)	p. 5
5. Atmospheric Conditions	pp. 5-9
6. ENSO Evolution	pp. 9-11
7. Summary	p. 12
8. References	p. 13

1. 2012 Seasonal Activity

The 2012 Atlantic hurricane season (Fig. 1) produced 19 named storms (NS), of which 10 became hurricanes (H) and two became major hurricanes (MH, maximum sustained surface wind speeds exceeding 111 mph or 178 km h⁻¹). The 1981-2010 seasonal averages are 12 named storms, 6 hurricanes, and 3 major hurricanes.

The seasonal Accumulated Cyclone Energy (ACE) value (Bell 2000) was 132.6×10^4 kt², which corresponds to 144% of the 1981-2010 median (Fig. 2). This value is the 19th highest since 1950, and the 11th highest in the last 30 years. Based on the ACE value, combined with above-

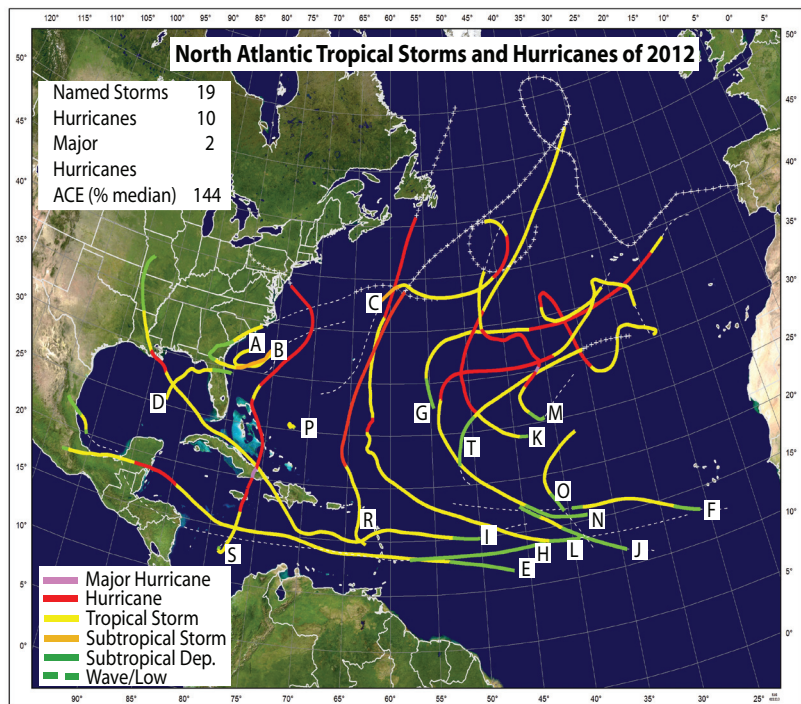


Fig. 1. Tracks of Atlantic named storms during 2012. Storm intensity is color-coded as shown at bottom left. Letters correspond to first initial of storm name.

average numbers of named storms and hurricanes, NOAA classifies the 2012 season as above normal.

This year marks the thirteenth above-normal season since the current high activity era for Atlantic hurricanes began in 1995 (Landsea et al. 1998; Goldenberg et al. 2001). During 1995-2012, 72% of seasons were classified as above normal, with eight (44%) being hyperactive (ACE exceeding 165% of the median), and only two seasons (11%) were below normal. These high levels of activity contrast sharply with the recent low-activity era of 1971-1994, when 12 (50%) seasons were below normal, and only three (12.5%) were above normal with none being hyperactive.

2. NOAA's Seasonal Hurricane Outlooks

NOAA's Climate Prediction Center (CPC) issues a pre-season Atlantic hurricane outlook in late May, and an updated outlook in early August to coincide with the peak months (August-October, ASO) of the season. Their predicted ACE ranges for 2012, with 70% probability of occurrence, had upper ACE bounds of 140% and 135%, respectively (red bars, Fig. 2), which were near the observed value of 144%. The observed number of major hurricanes (2) in 2012 was within NOAA's predicted ranges for both outlooks (Fig. 3).

However, each outlook indicated that a near-normal season strength was most likely (50% chance). Also, the predicted likely ranges (with 70% probability of occurrence) of named storms and hurricanes were below the observed levels.

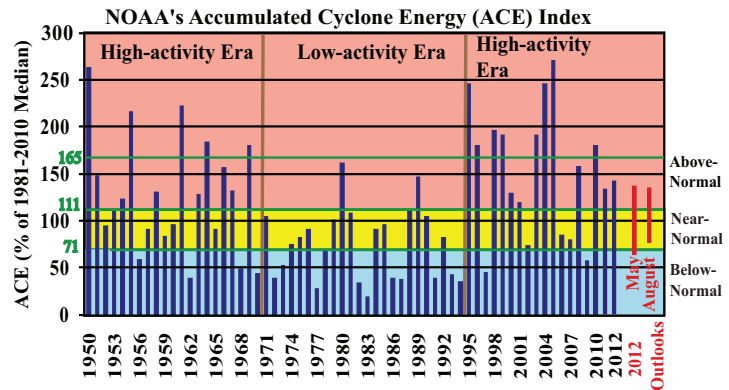


Fig. 2. NOAA's Accumulated Cyclone Energy (ACE) index expressed as percent of the 1981-2010 median value. ACE is calculated by summing the squares of the 6-hourly maximum sustained surface wind speed (knots) for all periods while the storm is at least tropical storm strength. Red bars show NOAA's predicted ACE ranges from their May and August seasonal hurricane outlooks. Pink, yellow, and blue shadings correspond to NOAA's classifications for above-, near-, and below-normal seasons, respectively. The 165% threshold for a hyperactive season is indicated. Vertical brown lines separate high- and low-activity eras.

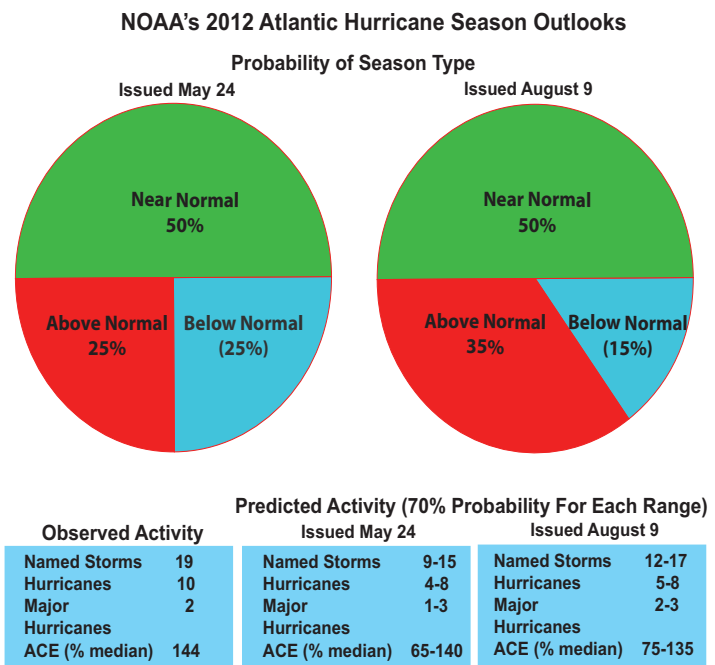


Fig. 3. NOAA's 2012 Atlantic hurricane season outlooks issued on 24 May and updated on 9 August. The observed seasonal activity is shown at bottom left.

These under-predictions largely reflected dynamical model forecasts (Figs. 4a, b) and the official CPC El Niño/ Southern Oscillation (ENSO) forecasts (Figs. 4c, d), which suggested that El Niño could develop in time to suppress hurricane activity during the latter half of the season.

For example, the average of the dynamical model forecasts (thick red line, Figs. 4a, b) issued in both May and August indicated that El Niño could form during July-September (JAS) or ASO and then persist into the upcoming winter. However, the average of the statistical model forecasts (thick green line) indicated that El Niño would not develop during the hurricane season.

Consistent with the dynamical model forecasts, the CPC ENSO forecast issued in May indicated a 40% probability that El Niño would occur during ASO 2012 (Fig. 4c), while the ENSO forecast issued in August increased this probability to 72% (Fig. 4d). These forecasts show that predictions of El Niño, La Niña, and their impacts, remain an ongoing scientific challenge facing climate scientists today. Error and uncertainty in such predictions directly impact the Atlantic hurricane season outlooks.

3. Atlantic Named Storm Tracks during 2012

August-October are typically the peak months of the season, and all but four NS (with one hurricane) formed during ASO 2012. In above-normal seasons, much of the ASO activity is linked to storms that first develop in the Main Development Region (MDR, green boxed region in Fig. 5), which spans the tropical Atlantic Ocean and Caribbean Sea between 9.5°N and 21.5°N (Goldenberg et al. 2001).

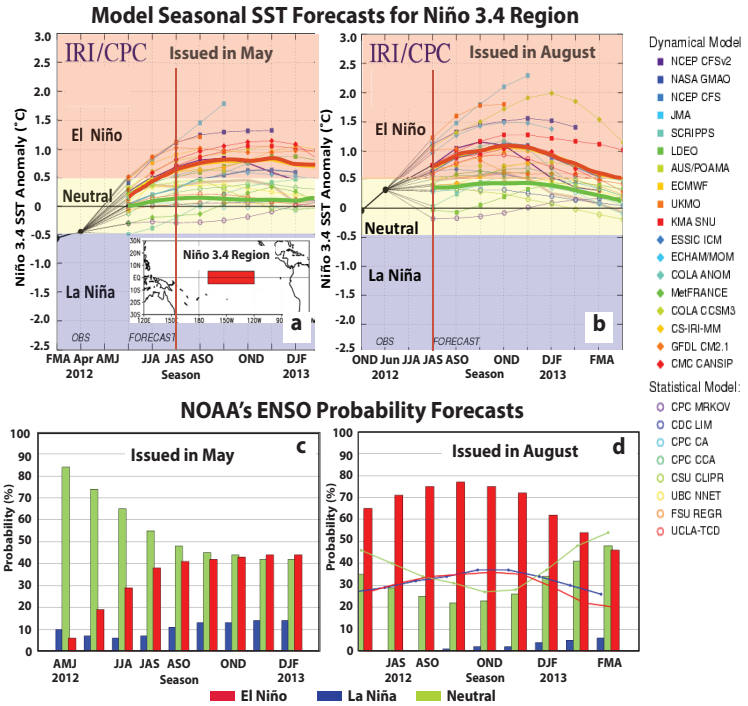


Fig. 4. Top: Model forecasts issued in (a) May and (b) August 2012, for SST anomalies in the Niño 3.4 region [inset of (a)]. Models are listed at right, with dynamical (statistical) models indicated by closed (open) markers and the respective model averages shown by thick red (green) line. Vertical brown line denotes the JAS season. Bottom (c, d): Corresponding NOAA ENSO forecasts showing probabilities for El Niño, La Niña, and Neutral (Red, blue, and green bars).

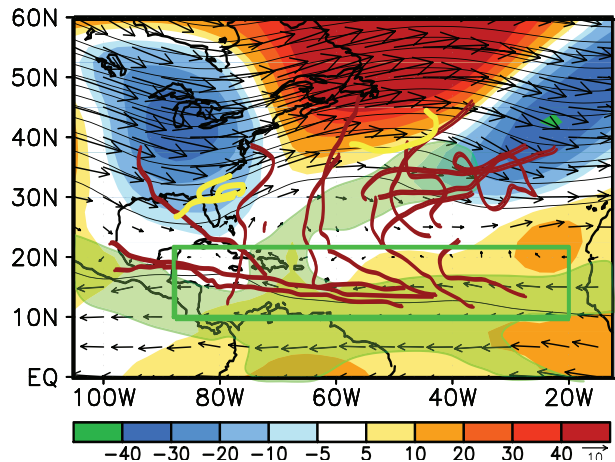


Fig. 5. ASO 2012: 500 hPa heights (contours, m) and anomalies (red/ blue shading), 600 – 300 hPa layer mean wind vectors ($m s^{-1}$), and 200-850 hPa vertical wind shear magnitude less than $8 m s^{-1}$ (green shading). Named storms (before) after 1 August are shown by yellow (brown) lines, beginning with tropical depression strength. Green box denotes the MDR. Vector scale is at right of color bar. Anomalies are with respect to the 1981-2010 period monthly means.

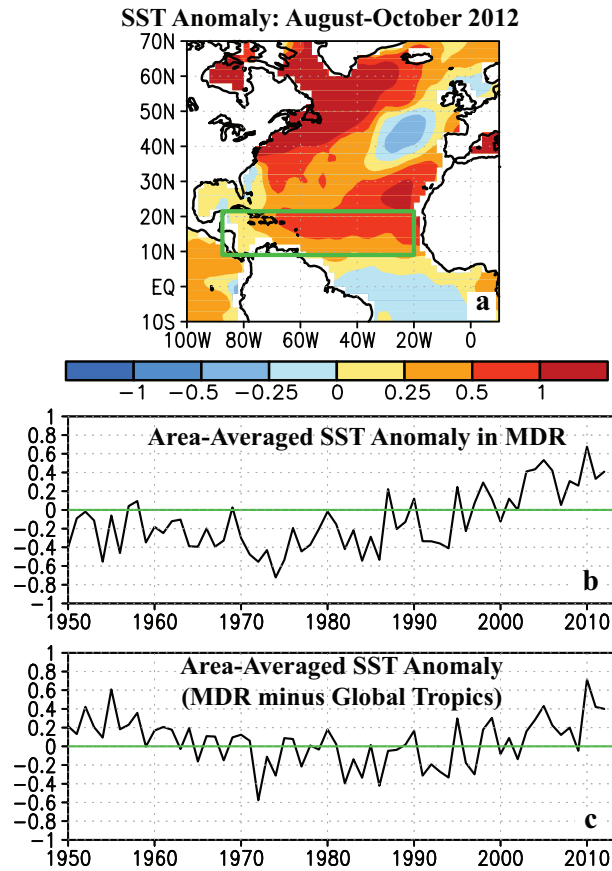


Fig. 6. (a) ASO 2012 SST anomalies ($^{\circ}\text{C}$). (b) Time series during 1950-2012 of ASO area-averaged SST anomalies in the MDR [green box in (a)]. (c) Time series showing the difference between ASO area-averaged SST anomalies in the MDR and those for the entire global tropics (30°N - 30°S). Anomalies are departures from the ERSST V3b (Smith et al. 2008) 1981-2010 period monthly means.

During 2012, the four named storms which formed prior to ASO were outside the MDR (yellow lines, Fig. 5). Of the 15 storms that formed during ASO (brown lines), nine developed within the MDR with six becoming hurricanes and one becoming a major hurricane (Sandy). These nine storms accounted for two-thirds of the seasonal ACE value. Three of the nine made landfall at hurricane strength, including Ernesto (Yucatan Peninsula), Isaac (Louisiana), and Sandy (Jamaica, Cuba as a MH, and New Jersey as a powerful extratropical storm).

This high level of activity within the MDR reflected weak vertical wind shear (green shading, Fig. 5) and above-average sea-surface temperatures (SSTs) (Fig. 6a) across much of that region. These conditions are typical of the ongoing high-activity era for Atlantic hurricanes (Fig. 7, see also Goldenberg et al. 2001; Bell and Chelliah 2006; Bell et al. 2011, 2012).

Also in 2012, two named storms formed over the Gulf of Mexico (Fig. 5). Debby made landfall in Florida as a tropical storm and Helene made landfall in Mexico as a tropical depression.

Eight named storms (four tropical storms and 4 H, with one becoming MH Michael) formed north of the MDR over the North Atlantic, and remained at sea. On average, 3-4 named storms per season form in this region, and

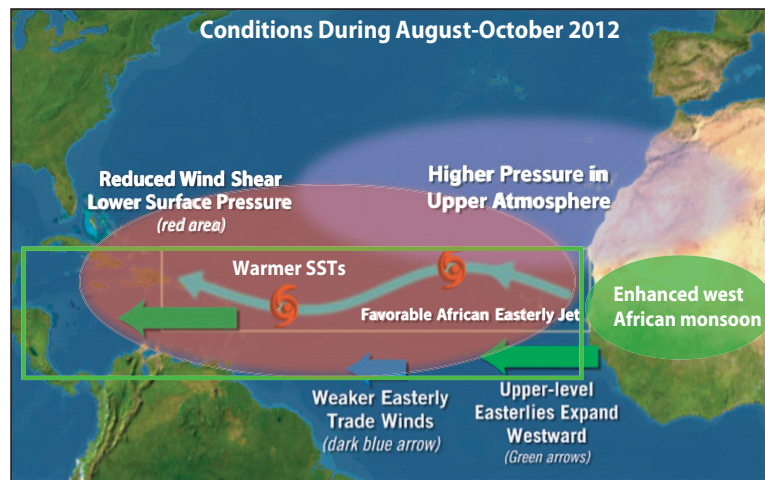


Fig. 7. Schematic depiction of atmospheric and oceanic conditions over the Atlantic basin during ASO 2012. Green box denotes the MDR. This inter-related set of conditions has been present since 1995.

roughly two become hurricanes. The increased activity north of the MDR during 2012 reflected a strong mid- and upper-level ridge across the subtropical North Atlantic, along with an extensive region of weak vertical wind shear (Fig. 5) and anomalously warm SSTs (Fig. 6a).

These conditions were part of a larger-scale circulation pattern that also featured amplified troughs over the eastern U.S. and the eastern North Atlantic (Fig. 5). An eastern U.S. trough pattern, and its associated strong southwesterly steering flow over the western North Atlantic, was also present during ASO 2010 and ASO 2011 (Bell et al. 2011, 2012). In all three years, these conditions contributed to a large number of named storms that stayed well east of North America (Blake et al. 2011).

4. Atlantic Sea Surface Temperatures (SSTs)

Sea surface temperatures in the MDR were above average during ASO 2012, with the largest departures (between 0.5°C and 1.0°C) observed across the north-central and northeastern MDR (Fig. 6a). The mean SST departure within the MDR was +0.41°C (Fig. 6b), which is 0.40°C warmer than the average departure for the entire global tropics (Fig. 6c).

Atlantic warmth compared to the remainder of the global tropics is typically associated with increased Atlantic hurricane activity. This condition has generally been present since 1995 (Fig. 6c), in association with the warm phase of the AMO (Fig. 8) (Enfield and Mestas-Nuñez 1999; Goldenberg et al. 2001; Vecchi et al. 2008; Bell et al. 2011, 2012). It was observed during the previous warm AMO phase and increased Atlantic hurricane activity of the 1950's and 1960's. Conversely, the MDR was generally cooler than the global tropics during the cold AMO phase and reduced Atlantic hurricane activity of the 1970's through the early 1990's.

5. Atmospheric Conditions

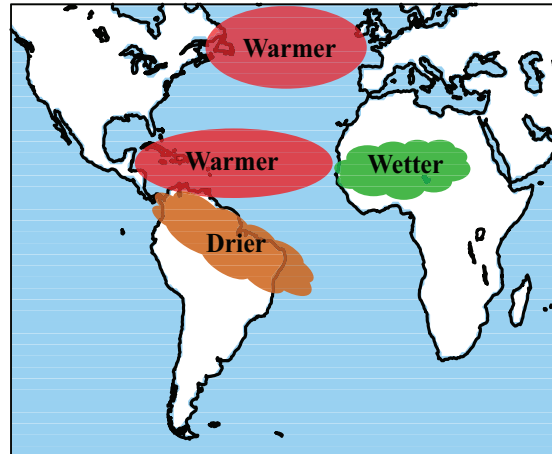


Fig. 8. Schematic depiction of the tropical multi-decadal signal and warm phase of the Atlantic Multi-decadal Oscillation (AMO) during 1995-2012, adapted from Bell and Chelliah (2006).

The transition in 1995 to a high activity era for Atlantic hurricanes reflected a phase change in the AMO and in the corresponding tropical multi-decadal signal (Goldenberg et al. 2001; Bell and Chelliah 2006; Bell et al. 2007). This signal links variability in the MDR to multi-decadal fluctuations in the AMO and in the west African monsoon (Fig. 8).

Consistent with this ongoing multi-decadal signal, the atmospheric circulation during ASO 2012 again featured an inter-related set of conditions known to be exceptionally conducive to tropical cyclone formation and intensification within the MDR (Fig. 7) (Goldenberg and Shapiro 1996; Landsea et al. 1998; Goldenberg et al. 2001; Bell and Chelliah 2006; Kossin and Vimont 2007; Bell et al. 2012). Similar ASO conditions have been present throughout the period 1995-2012.

A yearly archive of these conditions can be found at the CPC web site (<http://www.cpc.ncep.noaa.gov/products/outlooks/hurricane-archive.shtml>) and in the *State of the Climate* reports that appear annually in the *Bulletin of the American Meteorological Society* (e.g., Bell et al. 2013).

Some of these inter-related conditions during

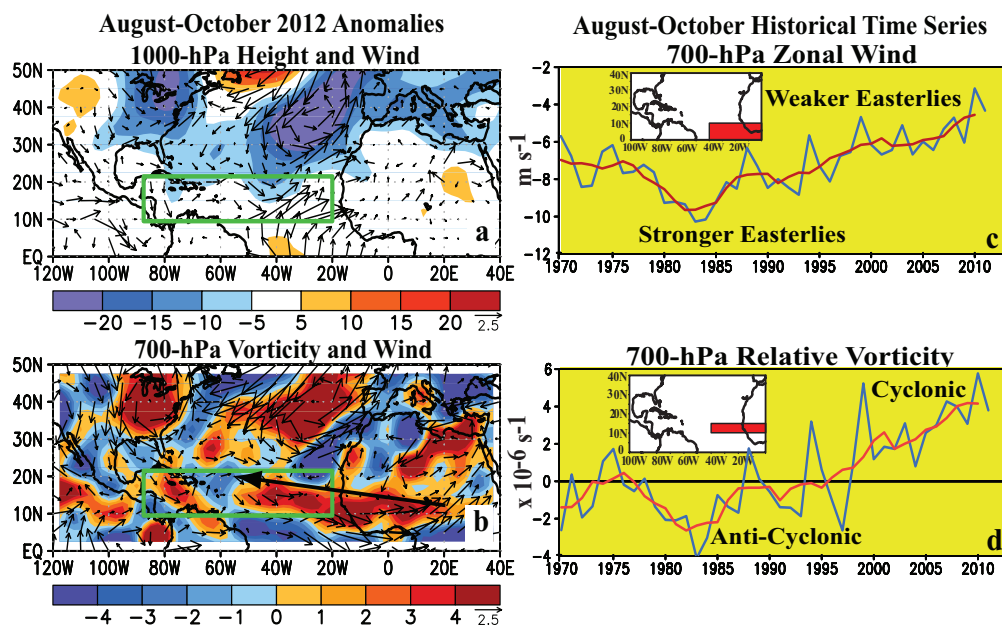


Fig. 9. (Left) ASO 2012 anomalies: (a) 1000-hPa heights (m) and wind vectors (m s^{-1}), and (b) 700-hPa relative vorticity ($\times 10^{-6} \text{ s}^{-1}$) and wind vectors, with thick arrow showing mean African Easterly Jet (AEJ). Green boxes denote MDR. Anomalies are departures from the 1981-2010 period monthly means. (Right) Time series showing ASO values of 700-hPa area-averaged (c) zonal wind and (d) relative vorticity. Blue (red) curve shows un-smoothed (5-pt running mean) values. Insets show averaging regions (Red).

ASO 2012 are shown (Figs. 9-11). In the lower atmosphere, below-average heights and surface pressure were evident to the north of the MDR (blue shading). Westerly/ south-westerly wind anomalies, indicating weaker trade winds and enhanced cross-equatorial flow, were present across the MDR (Fig. 9a). The westerly wind anomalies extended above 700-hPa, the level of the African Easterly Jet (AEJ, Fig. 9b), and were associated with an anomalous northward shift of the AEJ core (thick black arrow).

As a result, the bulk of the African easterly wave energy (Reed et al. 1977) was often centered well within the MDR. The AEJ also featured increased cyclonic shear along its equator-ward flank (red shading, Fig. 9b), which dynamically favors stronger easterly waves. These conditions are opposite to those seen during 1971-1994 (Figs. 9c, d).

Also during ASO 2012, enhanced upper-level ridges spanned the subtropical Atlantic and Africa in both hemispheres (Fig. 10a). This inter-hemispheric symmetry is consistent

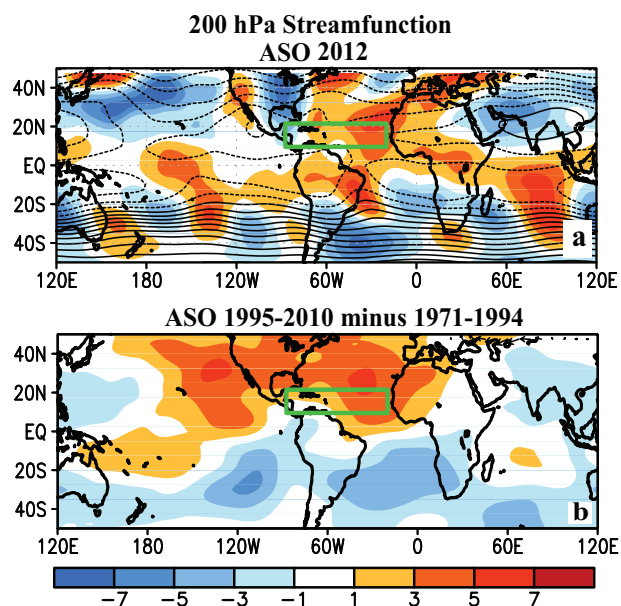


Fig. 10. 200 hPa streamfunction; (a) total (contours, interval is $10 \times 10^6 \text{ m}^2 \text{ s}^{-1}$) and anomalies during ASO 2012, and (b) difference between the 1995-2010 and 1971-1994 ASO means. Anomalous ridges are shown red (blue) in the NH (SH). Anomalous troughs are shown blue (red) in the NH (SH). Green boxes denote the MDR. Anomalies are with respect to the 1981-2010 period monthly means.

**Anomalous Velocity Potential and Divergent Wind
ASO 2012**

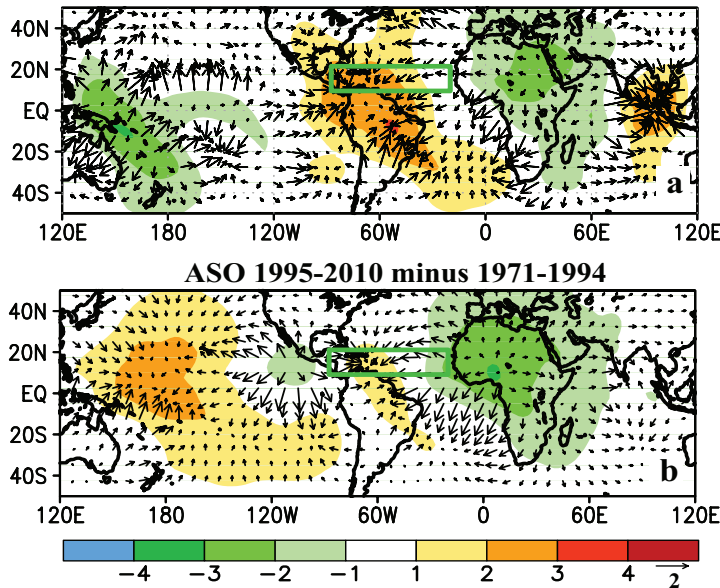


Fig. 11. 200 hPa (a) anomalous velocity potential (shading, $\times 10^6 \text{ m}^2 \text{ s}^{-1}$) and divergent wind vectors (m s^{-1}) during ASO 2012, and (b) difference between the 1995-2010 and 1971-1994 ASO means. Vector scale is at right of color bar. Green boxes denote the MDR. Anomalies are with respect to the 1981-2010 period monthly means.

with an enhanced west African monsoon system (Fig. 11a), both of which are prominent features of the Atlantic high activity era (Figs. 10b, 11b).

In addition to weaker trade winds, these conditions contributed to anomalous upper-level easterly flow across the MDR. The result was weaker vertical wind shear (orange shading, Fig. 12a) resulting from anomalous easterly shear across the MDR, similar to that which has prevailed since 1995 (Fig. 12b).

These conditions were part of a larger-scale pattern that included increased shear over both the eastern equatorial Atlantic and the eastern tropical North Pacific (blue shading, Fig. 12a), which is also typical of other above-normal seasons since 1995 (Bell and Chelliah 2006; Bell et al. 2011).

The question then arises as to why there was so little major hurricane activity in 2012. Only two 6-hourly periods were observed with storms at MH strength, which corresponds to one-half of a major hurricane day (MHD). [The measure Major Hurricane Days, or

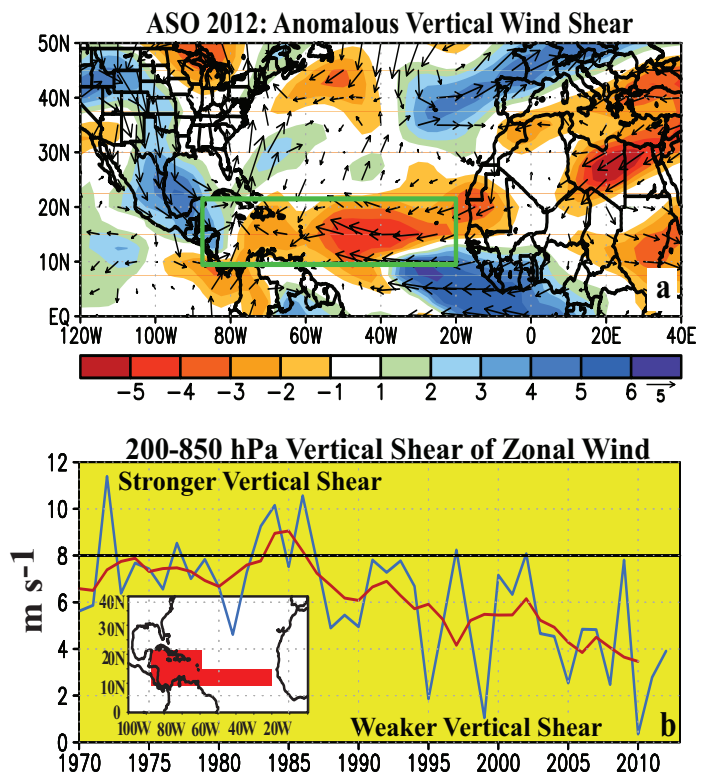


Fig. 12. (a) ASO 2012 anomalous vertical wind shear magnitude and vectors (m s^{-1}). Green box denotes the MDR. Vector scale is at right of color bar. Anomalies are with respect to the 1981-2010 period monthly means. (b) Historical time series showing yearly ASO values of area-averaged vertical shear of the zonal wind. Blue (red) curve shows un-smoothed (5-pt running mean) values. Inset shows averaging region (Red).

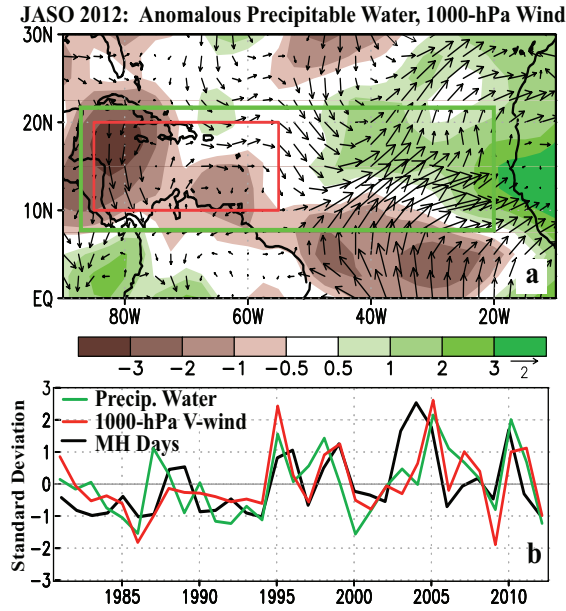


Fig. 13. (a) July-October (JASO) 2012 anomalous precipitable water (mm) and 1000 hPa vector winds (m s^{-1}). Green box denotes the MDR and red box denotes averaging region for (b). Vector scale is at right of color bar. (b) June-November standardized anomalies of MH days (black line), and JASO standardized anomalies of area-averaged precipitable water (green line) and meridional (V-) component of 1000 hPa wind (red line), for red boxed region shown in (a). Anomalies are with respect to the 1981-2010 period monthly means.

Intense Hurricane Days (IHD, Gray et al. 1993), is the sum of all 6-hourly periods that storms were at MH status, with each period counting as 0.25 MHD.]

The 2012 MHD value is the lowest since 1995, and is lower than for 79% of the years during 1971-1994. Two reasons for the low 2012 MH activity are: (1) Many storms remained over the central North Atlantic in an area of relatively cool SSTs throughout their life (Fig. 1) ; and (2) Only two of five named storms over the Caribbean Sea became hurricanes (Ernesto and Sandy) and each made landfall shortly thereafter.

This low MH activity over the Caribbean Sea was partly related to anomalous dry air (brown shading, Fig. 13a) and northerly low-level winds during Jul.-Oct. (JASO). There is a

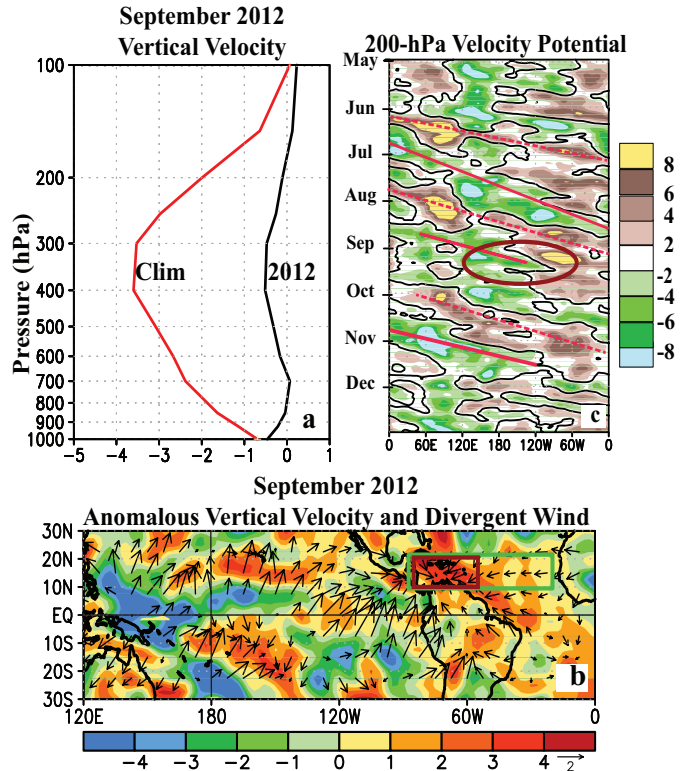


Fig. 14. (a) Sep. 2012 atmospheric vertical profile of area-averaged total (black curve) and anomalous (red curve) vertical velocity ($\times 10^2 \text{ hPa s}^{-1}$) over the Caribbean Sea [red boxed region, panel (b)], (b) Sep. 2012 anomalies of 500 hPa vertical velocity and 200 hPa divergent wind vectors (m s^{-1}). In (a, b), positive (negative) values indicate descending (ascending) air. (c) Equatorial time-longitude section showing 5-day running mean of anomalous 200 hPa velocity potential ($\times 10^6 \text{ m}^2 \text{ s}^{-1}$) averaged between 2°N - 2°S . Green (brown) shading shows anomalous rising (sinking) air. Red lines show MJO episodes. Brown circle shows September conditions. Anomalies are departures from the 1981-2010 base period daily means.

strong historical relationship between increased (decreased) hurricane activity, increased (decreased) moisture, and southerly (northerly) low-level wind anomalies (Fig. 13b).

Conditions were especially non-conducive to MH formation over the Caribbean Sea during September 2012, when there was a complete disappearance of the normal ascending motion throughout the lower and middle troposphere (black curve in Fig. 14a, see also Klotzbach and Gray 2012).

This record anomalous sinking motion was linked to a larger-scale pattern (Fig. 14b)

featuring anomalous ascending motion and upper-level divergence over the equatorial Pacific near the date line, and anomalous descending motion and upper-level convergence across the MDR. This overall pattern reflected a quasi-stationary intra-seasonal fluctuation in tropical convection (brown circle, Fig. 14c) that appeared to be reinforced by an active Madden-Julian Oscillation (MJO, red lines).

Despite the limited MH activity during 2012, the analysis indicates that all key inter-related features of the active Atlantic phase of the tropical multi-decadal signal and AMO were again present during the hurricane season (Figs. 6-11). Therefore, there is no apparent weakening of the conducive conditions that have prevailed since 1995, nor is there any evidence to suggest that the current high-activity era for Atlantic hurricane activity might be ending.

6. ENSO Evolution

El Niño and La Niña are opposite phases of ENSO, and can strongly influence Atlantic hurricane activity (Gray 1984, Bell and Chelliah 2006). NOAA classifies these phenomena using the Niño-3.4 index (Fig. 15a), which is based on the area-averaged SST anomalies (using the ERSST-V3b data set of Smith et al. 2008) in the east-central equatorial Pacific between 5°N-5°S, 170°W-120°W (black box, Fig. 16).

The Oceanic Niño Index (ONI) is a 3-month running average of the Niño-3.4 index (Fig. 15b). The ONI is used to monitor and predict ENSO in real time, and to classify El Niño and La Niña events historically. The CPC classifies El Niño (La Niña) when the ONI is greater-(less-) than or equal to +0.5°C (-0.5°C) for five consecutive overlapping seasons.

In 2012, the Niño 3.4 index became increasingly positive as the summer and fall progressed, exceeding +0.5°C during September and November (Fig. 15a). The resulting ONI exceeded the lower threshold for El Niño (+0.5°C) during ASO and September-

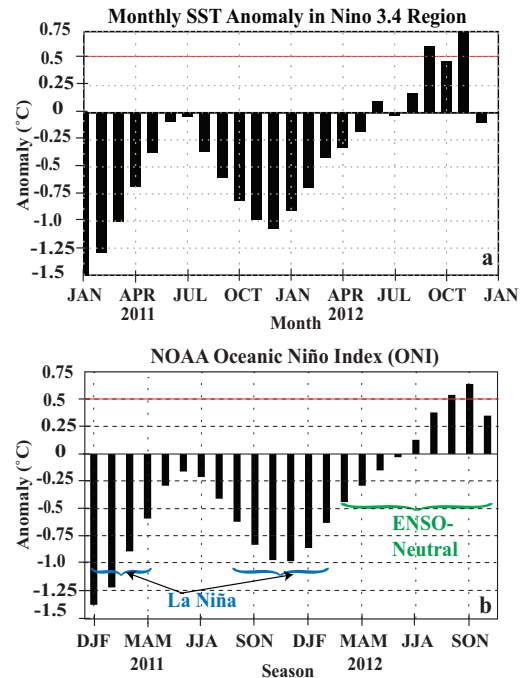


Fig. 15. (a) Time series of monthly area-averaged SST anomalies in the Niño 3.4 region [see black box, Fig. 16], and (b) NOAA's Oceanic Niño index (ONI), for consecutive 3-month running seasons. Red lines indicate the +0.5°C values. SST anomalies are departures from the 1981-2010 period monthly means. Adapted from Halpert et al. (2013).

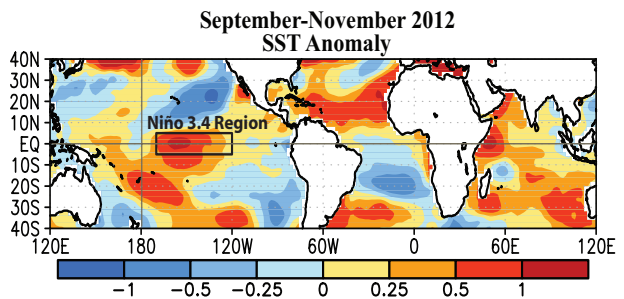


Fig. 16. SST anomalies (°C) during September-November (SON) 2012. Black box denotes the Niño 3.4 region. Anomalies are departures from the 1981-2010 period monthly means using the ERSST V3b data set (Smith et al. 2008).

November (SON). During SON, the largest positive SST anomalies exceeded +1.0°C, and were observed in the western part of the Niño 3.4 region (Fig. 16).

However, this warmth subsequently dissipated during December and the Niño 3.4 index became negative (Fig. 15a). This abrupt

**Equatorial (2°N-2°S) Time-Longitude Sections for Pacific Basin
May-December 2012**

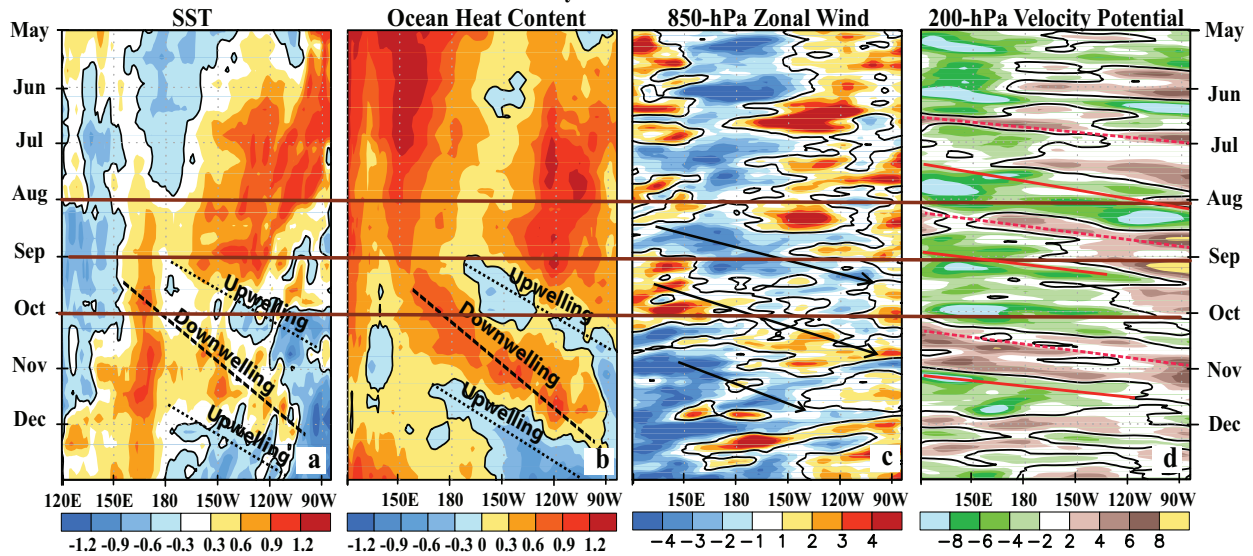


Fig. 17. Equatorial (2°N-2°S) Pacific Ocean time-longitude sections of anomalies during May-December 2012: (a) pentad sea surface temperatures (°C), (b) pentad upper ocean (0-300 m) heat content (°C), (c) 5-day running mean 850 hPa zonal wind (m s^{-1}), and (d) 5-day running mean 200 hPa velocity potential ($\times 10^6 \text{ m}^2 \text{ s}^{-1}$). Horizontal brown lines show August and September. In (a, b) dashed (solid) lines show downwelling (upwelling) equatorial oceanic Kelvin waves. In (c), blue (orange) shading indicates easterly (westerly) anomalies, and arrows show intra-seasonal variability. In (d) green (brown) shading shows areas of anomalous rising (sinking) air, and red lines show the main MJO episodes. In all panels, thick brown lines highlight the months of August and September. Anomalies are departures from the 1981-2010 base period means.

end to a developing El Niño is unprecedented in the historical record dating to 1950 (Halpert et al. 2013).

As noted in section 2, NOAA’s overall under-prediction of the 2012 Atlantic hurricane season reflected an expectation that El Niño could develop in time to suppress the seasonal hurricane activity. However, the ONI exceeded the El Niño threshold for only two consecutive overlapping seasons (Fig. 15b), which is insufficient to be classified as El Niño.

Several inter-related factors prevented El Niño from developing as the late-summer and fall progressed. These factors are described within the context of the overall evolution of the equatorial Pacific SST and oceanic heat content anomalies, and the overall tropical convection and low-level wind anomalies (Fig. 17).

During May-August, typical features of a developing El Niño included an expanding and strengthening pattern of above-average SSTs

and above-average oceanic heat content across the east-central and eastern equatorial Pacific (Figs. 17a, b). Also, the equatorial easterly trade winds were weaker than average in these regions (orange shading, Fig. 17c). However, no apparent link was yet evident between the SST warming and enhanced tropical convection, as convection was generally suppressed east of the date line (brown shading, Fig. 17d).

During SON, the SST anomalies continued to warm in the Niño 3.4 region. However, no additional warming occurred below the ocean surface, and no additional expansion or strengthening of the westerly trade wind anomalies was evident, as would be expected if El Niño were to develop further.

Instead, the heat content and trade wind anomaly patterns rapidly lost, and never regained, their El Niño-like structure, as indicated by transitions in the anomaly patterns from ones of persistence during May- mid August

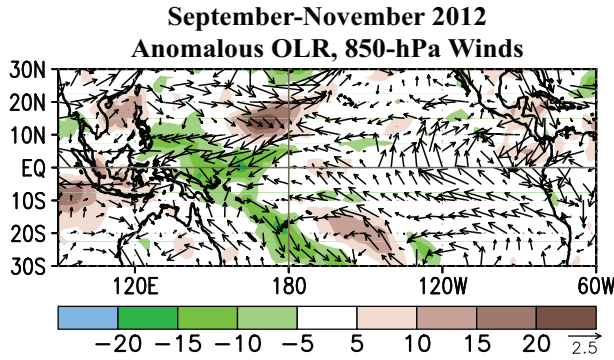


Fig. 18. September-November (SON) anomalies of Outgoing Longwave Radiation (OLR) (shading, $W m^{-2}$) and 850 hPa wind vectors ($m s^{-1}$). Green (brown) shading in tropics indicates enhanced (suppressed) convection. Vector scale is at right of color bar. Anomalies are departures from the 1981-2010 period monthly means.

to ones of transience and strong intra-seasonal variability during September-December (Figs. 17b, c). In the atmosphere, this intra-seasonal variability was related to the MJO, while in the ocean it was related to a series of equatorial oceanic Kelvin waves (see also Gottschalck and Bell 2013).

These intra-seasonal phenomena prevented El Niño from developing in at least two ways. First, long periods of easterly wind anomalies were present during Aug.-Sep. and Nov.-Dec. in association with the MJO (Fig. 17c). For the SON season as a whole, the trade winds were enhanced across most of the Pacific basin (even as SSTs warmed in the Niño 3.4 region) and convection remained enhanced well west of the date line (Fig. 18). This lack of an organized atmospheric response to the anomalous SST warming meant that the ocean-atmosphere interactions necessary for El Niño to develop and persist were largely absent during this critical period in its evolution.

Second, the MJO-related trade wind variability contributed to a series of strong equatorial oceanic Kelvin waves (Fig. 17b), which dominated the sub-surface thermocline and temperature anomalies beginning in September. Two upwelling Kelvin waves,

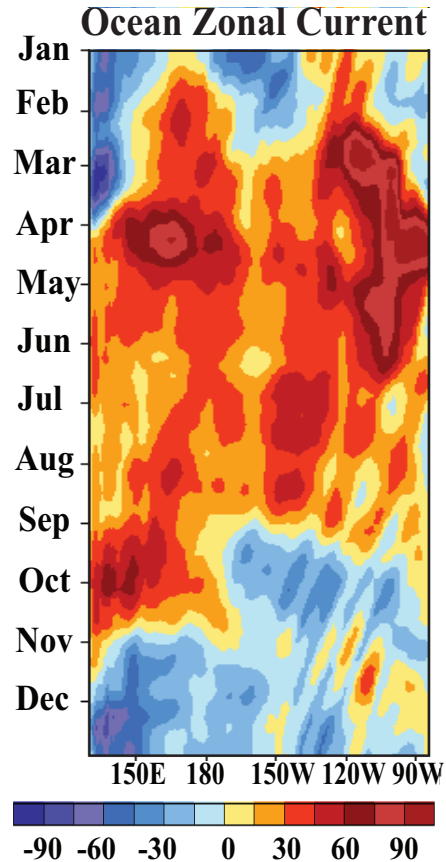


Fig. 19. Equatorial ($2^{\circ}N-2^{\circ}S$) Pacific Ocean time-longitude section during 2012 of anomalous upper ocean (15 m depth) zonal current ($cm s^{-1}$). Blue shading indicates easterly anomalies and a stronger westward current. Orange shading indicates westerly anomalies and a weaker westward current. Anomalies are departures from the 1981-2010 GODAS base period pentad means.

strengthened in the presence of the strong easterly trade winds (Roundy and Kiladis 2006), cooled the upper ocean during September- early October and again in December. These upwelling waves directly contributed to a collapse of the oceanic thermal structure necessary for El Niño to develop and persist. This collapse occurred in part through 1) an enhanced westward surface zonal ocean current (blue shading, Fig. 19) which transported anomalously warm water out of the Niño 3.4 region, and 2) eastern Pacific up-welling of cold sub-surface waters to the ocean surface (Fig. 17a).

7. Summary

The above-normal 2012 Atlantic hurricane season resulted from an inter-related set of atmospheric and oceanic anomalies that have been present during ASO since the onset of the current high activity era in 1995. The observations provide no indication that this high activity era for Atlantic hurricanes has ended, and there is no indication of a weakening or disappearance of the conditions responsible for the it.

The atmospheric and oceanic conditions during the 2012 hurricane season showed strong links to two inter-related climate factors: the tropical multi-decadal signal and the warm phase of the AMO. These climate signals have been present since 1995. They were again associated with an enhanced west African monsoon system, warmer SSTs, and weaker easterly trade winds across the MDR, along with reduced vertical wind shear and conducive winds that strengthen storms moving westward from Africa. This inter-related set of conditions is very conducive to Atlantic hurricane activity.

Despite the large numbers of named storms and hurricanes during 2012, only two 6-hourly periods were observed with storms at MH strength. Some reasons for this low MH activity are evident. First, many storms remained over the central North Atlantic in an area of relatively cool SSTs throughout their life. Second, of the five named storms that moved over the Caribbean Sea, only two became hurricanes (Ernesto and Sandy) and each made landfall shortly thereafter. It is seen that exceptionally dry air and record anomalous sinking motion (in September) suppressed hurricane activity over the Caribbean Sea.

Overall, NOAA under-predicted the strength of the 2012 hurricane season, largely because of an expectation that El Niño could develop in time to suppress tropical storm and hurricane activity. However, El Niño failed to develop, despite an evolution during June-

August which suggested that such development was imminent.

The observations show that strong intra-seasonal variability during September through December in both the atmosphere (*via* the MJO) and ocean (*via* two upwelling equatorial oceanic Kelvin waves) played a crucial role in preventing El Niño from forming.

This intra-seasonal variability appears to have prevented El Niño's development in at least two ways. First, the MJO produced long periods of enhanced easterly trade winds, along with a westward displacement of the enhanced convection relative to the anomalously warm SSTs. These conditions meant that the ocean-atmosphere interactions necessary for El Niño to develop and persist were largely absent. Second, two upwelling equatorial oceanic Kelvin waves were strengthened, in response to the enhanced easterly trade winds. These waves ultimately destroyed, *via* a combination of advection and upwelling, the necessary surface and sub-surface thermal structure required for El Niño to develop and persist.

The average of the dynamical model forecasts issued in both May and August indicated that El Niño would form during July-September, and then persist into the upcoming winter. The above analysis suggests that these forecast errors are related to known model shortcomings in many dynamical models regarding monthly and seasonal predictions of the MJO and equatorial oceanic Kelvin wave activity.

Interestingly, many statistical models at the time accurately predicted that El Niño would not develop by ASO. However, no statistical seasonal ENSO prediction model currently incorporates the MJO and oceanic Kelvin wave activity, which as seen above helped prevent El Niño from developing. Predictions of El Niño, La Niña, and their impacts, remain an ongoing scientific challenge facing climate modelers, forecasters, and scientists.

8. References

- Bell, G. D., 2000: The 1999 North Atlantic Hurricane Season: A Climate Perspective. *Climate Assessment for 1999. Bull. Amer. Meteor. Soc.*, **81**, S19-S23.
- Bell, G. D., and co-authors, 2007: The 2006 North Atlantic Hurricane Season: A Climate Perspective. *State of the Climate in 2006*. D A. Arguez, Ed. *Bull. Amer. Meteor. Soc.*, **88**, S48-S51.
- Bell, G. D., and co-authors, 2011: The 2010 Atlantic Hurricane Season: A Climate Perspective. *State of the Climate in 2010*. J. Blunden, D. S. Arndt and M. O. Baringer, Eds. *Bull. Amer. Meteor. Soc.*, **92**, S115-S121.
- Bell, G. D., and co-authors, 2012: The 2011 North Atlantic Hurricane Season: A Climate Perspective. *State of the Climate in 2011*. J. Blunden and D. S. Arndt, Eds. *Bull. Amer. Meteor. Soc.*, **93**, S99-S105.
- Bell, G. D., and co-authors, 2013: The 2012 North Atlantic Hurricane Season: A Climate Perspective. *State of the Climate in 2011*. J. Blunden and D. S. Arndt, Eds. *Bull. Amer. Meteor. Soc.*, **94**, In Press.
- Bell, G. D., and M. Chelliah, 2006: Leading tropical modes associated with interannual and multi-decadal fluctuations in North Atlantic hurricane activity. *J. Climate*, **19**, 590-612.
- Blake, E., C. W. Landsea, and E. J. Gibney, 2011: The deadliest, costliest, and most intense United States tropical cyclones from 1851 to 2010. NOAA Technical Memorandum NWS NHC-6, NOAA National Hurricane Center. Dept. of Commerce (Available at http://www.nhc.noaa.gov/Deadliest_Costliest.shtml).
- Enfield, D. B., and A. M. Mestas-Nuñez, 1999: Multi-scale variabilities in global sea surface temperatures and their relationships with tropospheric climate patterns. *J. Climate*, **12**, 2719-2733.
- Goldenberg, S. B., C. W. Landsea, A. M. Mestas-Nuñez, and W. M. Gray, 2001: The recent increase in Atlantic hurricane activity: Causes and implications. *Science*, **293**, 474-479.
- Goldenberg, S. B., and L. J. Shapiro, 1996: Physical mechanisms for the association of El Niño and West African rainfall with Atlantic major hurricane activity. *J. Climate*, **9**, 1169-1187.
- Gottschalck, J., and G. D. Bell, 2013: Tropical intra-seasonal activity during 2012. *State of the Climate in 2012*. J. Blunden and D. S. Arndt, Eds. *Bull. Amer. Meteor. Soc.*, **94**, in Press.
- Gray, W. M., 1984: Atlantic seasonal hurricane frequency: Part I: El Niño and 30-mb quasi-biennial oscillation influences. *Mon. Wea. Rev.*, **112**, 1649-1668.
- Gray, W. M., C. W. Landsea, P. W. Mielke, Jr., and K. J. Berry, 1993: Predicting Atlantic basin tropical cyclone activity by 1 August. *Wea. Forecasting*, **8**, 73-86.
- Halpert, M., G. D. Bell, and M. L'Heureux, 2013: ENSO and the tropical Pacific. *State of the Climate in 2012*. J. Blunden and D. S. Arndt, Eds. *Bull. Amer. Meteor. Soc.*, **94**, in Press.
- Kossin, J. P., and D. J. Vimont, 2007: A more general framework for understanding Atlantic hurricane variability and trends. *Bull. Amer. Meteor. Soc.*, **88**, 1767-1781.
- Klotzbach, P. J., and W. M. Gray, 2012: Summary of 2012 Atlantic tropical cyclone activity and verification of author's seasonal and two-week forecasts. Dept. of Atmos. Sci., Colorado State Univ., 79 pp.
- Landsea, C. W., G. D. Bell, W. M. Gray, and S. B. Goldenberg, 1998: The extremely active 1995 Atlantic hurricane season: Environmental conditions and verification of seasonal forecasts. *Mon. Wea. Rev.*, **126**, pp. 1174-1193.
- Reed, R. J., D. C. Norquist, and E. E. Recker, 1977: The structure and properties of African wave disturbances as observed during Phase III of GATE. *Mon. Wea. Rev.*, **105**, 317-333.
- Roundy, P. E., and G. N. Kiladis, 2006: Observed Relationships between Oceanic Kelvin Waves and Atmospheric Forcing. *J. Climate*, **19**, 5253-5272.
- Vecchi, G. A., K. L. Swanson, and B. J. Soden, 2008. Whither Hurricane Activity? *Science*, **322** (5902), 687. DOI: 10.1126/Science.1164396